Desalination and Water Treatment
www.deswater.com

doi:10.5004/dwt.2017.20761

73 (2017) 249–255
April

Maximising flux in direct contact membrane distillation using nanofibre membranes

Tomáš Jiříček[a,b], Michal Komárek[b], Jiří Chaloupek[b], Tomáš Lederer[b]

[a]*Membrain s.r.o, Pod Vinicí 87, 47127 Stráž pod Ralskem, Czech Republic, Tel. +420 487 805 239, +420 485 351 111, email: tomas.jiricek@membrain.cz (T. Jiříček)*
[b]*Technical University of Liberec, Studentská 1402/2, 46117 Liberec 1, Czech Republic, Tel. +420 485 353 575, email: michal.komarek@tul.cz (M. Komárek), Tel. +420 485 353 247, email: jiri.chaloupek@tul.cz (J. Chaloupek), Tel. +420 485 353 638, email: tomas.lederer@tul.cz (T. Lederer)*

Received 26 July 2016; Accepted 26 March 2017

ABSTRACT

Electrospun PVDF nanofibre membranes were manufactured and tested on a direct-contact membrane distillation (DCMD) unit in an effort to maximise flux rate, which is generally low using standard MD membranes. In addition, membrane performance was compared with that of commonly available PTFE, PE and PES film membranes. Salt retention in all but one membrane was above 99 %. At high recirculation velocities, very thin nanofibre layers had up to 30 % higher flux rates than the best reference membranes, though it came at the cost of higher energy losses through conduction. Considering that DCMD is the least energy efficient configuration, nanofibre membranes show a promising future for MD applications with high flux rates. We suggest that new membranes be developed with specific target applications in mind, addressing specific module and operational conditions.

Keywords: Membrane distillation; Direct contact membrane distillation; DCMD; Nanofibres; Polyvinylidene fluoride; Flux enhancement

1. Introduction

New technologies for the desalination of sea and brackish water are constantly being developed and tested. At present, most demand is covered by established technologies such as high capacity reverse osmosis (RO); however, there are increasing concerns over issues related to energy consumption and brine disposal. In response to the growing demands for sustainable desalination, MD is rapidly gaining in popularity as it offers a number of advantages. Unlike pressure driven processes, MD can achieve a feed solution saturation level without any significant decline in flux. Moreover, the process can be driven using low-grade heat sources, including solar and geothermal energy or "waste" heat from wastewaters [1]. Unfortunately, MD performance is still inferior to that of traditional desalination technologies, both in terms of flux and energy efficiency [2]; hence, there have been few large MD applications as yet around the world, mostly due to the unavailability of suitable hydrophobic membranes. Commercially available film membranes for MD are mainly made of PP, PTFE, PVDF and PE [3]. Structurally, they are microfiltration membranes with a hydrophobic surface. Despite this, they still suffer from pore wetting as their structure is optimised for removal of bacteria and suspended particles from water, rather than temperature-driven liquid-vapour separation.

MD is a relatively complex process and an "ideal" membrane has to deal with a number of seemingly incompatible requirements, i.e.:

- high flux rates, provided by thin membranes with larger pores;
- low heat loss, provided by thick membranes with smaller pores; and
- excellent hydrophobicity, provided by membranes with uniform pore size and a high contact angle [4,5].

*Corresponding author.

Presented at the EDS conference on Desalination for the Environment: Clean Water and Energy, Rome, Italy, 22–26 May 2016.

Recent studies have suggested that the optimum membrane thickness should lie between 30 and 60 μm [6] and that the optimum pore size ranges between 0.1 to 1 μm [7].

The latest generation of membrane technology is represented by electrospun nanofibre membranes, which offer significantly higher flux rates at similar rejection rates to conventional membranes [8–10]. Moreover, there is no transmembrane hydrostatic pressure in temperature-driven MD; hence, the membranes do not need excessive mechanical strength, as is required during pressure-driven processes [11]. Low mechanical strength is one of the drawbacks of membranes with very high porosity; and yet this is one of the most desirable parameters for high flux and energy efficiency in all MD configurations [7,8,12–14]. A very high specific surface not only provides a large space for evaporation, it also reduces conductive heat loss across the nanofibre membrane due to the much lower thermal conductivity of the vapour-filled inner volume compared with the polymer layer [15].

In order to quatify these benefits, we undertook an experimental comparison between non-woven nanofibre membranes made from PVDF and commonly available film membranes made from PTFE, PE and PES. Testing included the varying of tangential velocity and feed concentration in order to investigate maximisation of membrane performance. Our results will expand on those of a previous study confirming the effectiveness of MD [16], by comparing different nanofibre membranes under a range of conditions and operational parameters, thereby deepening our understanding of how nonvowen membrane properties affect MD performance.

2. Materials and methods

2.1. Membranes

Nanofibre layers were prepared by continuous needleless electrospinning. This method produces thin filaments from polymer solutions using an electrostatic field as the main drawing force (Fig. 1). PVDF (Solef 1015, Solvay-Specialty polymers co.) and N,N-Dimethylformamide (Sigma-Aldrich) were both used as received. The polymer solution was prepared by dissolving the PVDF polymer in DMF, with polymer concentration set to 13 % w/w. The solution was stirred for five hours at 60°C on a magnetic stirrer in a sealed beaker to prevent solvent evaporation. The solution was then electrospun on a Nanospider™ needleless electrospinner (Elmarco) equipped with a 0.2 mm wire emitting/collecting electrode. The polymer solution is applied to the emitting electrode by a moving applicator and both electrodes are attached to a high voltage power supply. The potential difference applied causes charging of the polymeric solution, the charge on the surface inducing stretching forces that try to atomise the liquid. If the electrostatic forces overcome the capillary forces represented by surface tension, the polymeric solution is stretched into a "Taylor cone" and a liquid jet is emitted. The electrostatic field elongates the jet further and carries it toward a collecting electrode. The solvent evaporates during this process and the jet solidifies before reaching the collecting electrode. The voltage between electrodes was set at between 50 and 70 kV and the distance between electrodes was kept constant at 175 mm. Relative humidity in the electrospinning chamber

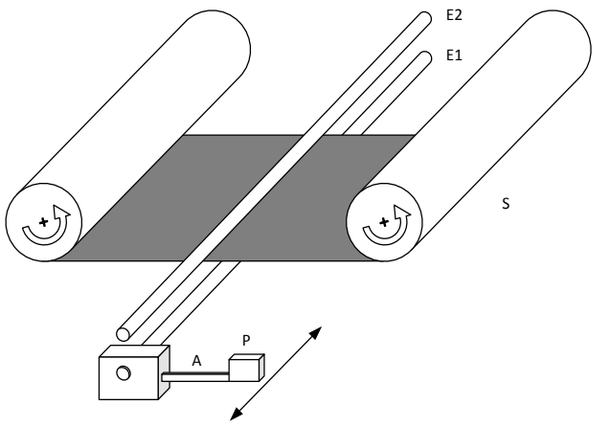

Fig. 1. Needleless electrospinning (A – applicator, P – polymer solution reservoir, S – substrate, E1 and E2 – wire electrode with applied voltage).

was kept below 40 % in order to minimise defect formation. Production speed varied according to the nanofibre membrane sheet thickness desired. The nanofibres were collected on a non-adhesive paper passing between the emitting and collecting electrodes, the speed of the passing substrate controlling the thickness of the membrane. The membranes were then laminated onto a nonwoven textile layer using a Meyer flatbed laminator set at 1.57 m min^{-1}, with a pressure of 10 N cm^{-2} and a temperature of 135°C.The nanofibre membranes were additionally coated with a bi-component PP/PE 70/30 spun bond support on either one or both sides.

A unique sample identification code was used relating the number of laminated spun bond layers, the polymer used and the membrane thickness. For example, 2PVDF139 is a two-side laminated PVDF membrane with a thickness of 13.9 μm. As fluoropolymers display excellent hydrophobicity, none of the membranes discussed in this paper were altered through the introduction of hydrophobic additives to the polymer solution.

Membrane performance was tested on a bench-scale DCMD experimental setup built around a flat sheet membrane module with an effective membrane area of 0.02 m^2. Membrane permeability testing was carried out using demineralised water in both circuits, while the retention tests used demineralised water in the distillate circuit and sodium chloride (NaCl) solution in the feed, concentration ranging from 0 to 100 g kg^{-1}. Circulation was counter-current with the position of the MD module flat and horizontal, the hot feed at the bottom and the cold distillate on top. Recirculation was powered through a peristaltic pump with a two-way rotational head using a cross-flow velocity of between 60 and 86 mm s^{-1}. The effect of feed concentration on flux and membrane retention was measured at 83 mm s^{-1}, corresponding with a mass flow rate of 1 kg min^{-1}. In all experiments, the logarithmic mean temperature difference (LMTD) was kept constant at 10°C, with the feed inlet temperature set at 50°C using two hot baths (Julabo F12 and Lauda RE 420). Temperatures were measured via four thermocouples set in the module inlet and outlet pipes.

Flux was calculated from the difference in mass on the feed and distillate A&D EK-12Ki scales. Electrical conduc-

tivity was measured via WTW TetraCon probes connected to WTW Mutli9430 and WTW Multi350i units. Retention was calculated as $R = 1 - c_d/c_f$, where c_f is the feed concentration and c_d is the distillate concentration. Energy efficiency, represented by the ratio of efficient heat by vapour flux and total heat transfer, was calculated as:

$$E = \frac{N\Delta HA}{mC_p\Delta T},$$

where N is flux, ΔH is the enthalpy of condensation, A is the membrane area, m is the mass flowrate along the membrane, C_p is the heat capacity and ΔT is the temperature difference at the inlet and outlet of the module. Data analysis was performed using GraphPad Prism6 and Microsoft Excel.

2.2. Porometry

Bubble point pressure and the maximum and average pore diameter were measured using a 3G POROMETER (Quantachrome), using the wet-dry flow method and Porefil as the wetting liquid.

2.3. Contact angle

Contact angle was measured with a THETA QC Optical Tensiometer (Attension) using demineralised water. Image analysis of the sample drop is carried out automatically and an average of the right and left angle provided.

2.4. Membrane structure and thickness

Membrane structure and thickness were calculated from a Tescan Vega3SB (Czech Republic) high vacuum scanning electron microscope (SEM) with an acceleration voltage of 30.0 kV. All samples were coated with a 5 nm thick layer of gold/palladium using a sputter coater (Quorum Technologies, England). Cross-sectional membrane thicknesses were obtained by cutting the membranes with a sharp razor and obtaining an image of the cut with the SEM. Tescan image analysis software (Tescan, USA) was used to measure nanofibre diameter and cross-sectional thickness.

3. Results and discussion

3.1. Membrane characterisation

The most obvious difference between the standard film membranes and the nanofibre layers was the membrane thickness, the latter (minus the supporting spun bond) being much thinner (Table 1). The pore size distribution was also different, with the nonwoven membranes apparently having larger pores. Note, however, that the nonwoven layers do not have pores as such, rather, the porometer assumes unitary tubular pores.

Membrane hydrophobicity is characterised by contact angle and bubble point pressure (see Table 1). Considering that PTFE membranes are renowned for their superb hydrophobicity, it was a great achievement to obtain contact angles in the same range in the PVDF layers. On the other hand, bubble point pressure was somewhat lower in the PVDF nanofibre layers. As there was no post-treatment on the laminated layers, and the two side-laminated membrane had the worst results, we suggest that the lamination step compromised otherwise excellent hydrophobicity in the PVDF layers.

SEM images of the membrane cross-sections clearly show compression from the razor cut in the PTFE, PE and PES film membranes (Fig. 2, top row). Images of the nanofibre membranes, on the other hand, clearly show the layer and its supporting layers, with 2PVDF139 having a supporting spun bond on both sides and 1PVDF155 and 1PVDF226 supported on one side only(Fig. 2, bottom row).

Structurally, the film membranes showed clear differences, with PTFE having the finest structure, PE rather large stretched shapes and PES small circular pores (Fig. 3). In comparison, the nanofibre layers were all structurally similar and all had a PVDF fibre diameter of around 200 nm. Overall structure was not uniform, however, with occasional polymer drops or fusing caused by non-evaporated DMF.

3.2. Flux

The demineralised water flux response to an increase in cross-flow velocity was similar in all membranes tested (Fig. 4A). Highest flux rates were observed for 1PVDF226 at all cross-flow velocities. Theoretically, the thinner 1PVDF155 layer should have had less resistance to mass transport; however it probably suffered from temperature polarisation which kept flux rates constantly lower than those for 1PVDF226. Layer 2PVDF139 had the lowest flux response, pore sizes greater than 0.3 µm apparently having no significant effect on flux increase [17]. Our results suggest that two-sided lamination greatly reduces membrane performance as 2PVDF139 had significantly lower flux rates at all cross-flow velocities, despite having almost the same thickness as 1PVDF155 (Fig. 4A).

Table 1
Membrane properties

Membrane	Lamination	Thickness (µm)	Mean pore (µm)	Maximum pore (µm)	Bubble point pressure (bar)	Contact angle
PTFE	–	72.1	0.22	0.276	2.320	136
PE	–	82.1	0.34	0.741	0.885	120
PES	–	72.5	0.55	0.620	1.303	131
2PVDF139	2 side	13.9	1.77	2.155	0.297	123
1PVDF155	1 side	15.5	1.07	1.364	0.469	135
1PVDF226	1 side	22.6	0.92	1.060	0.601	129

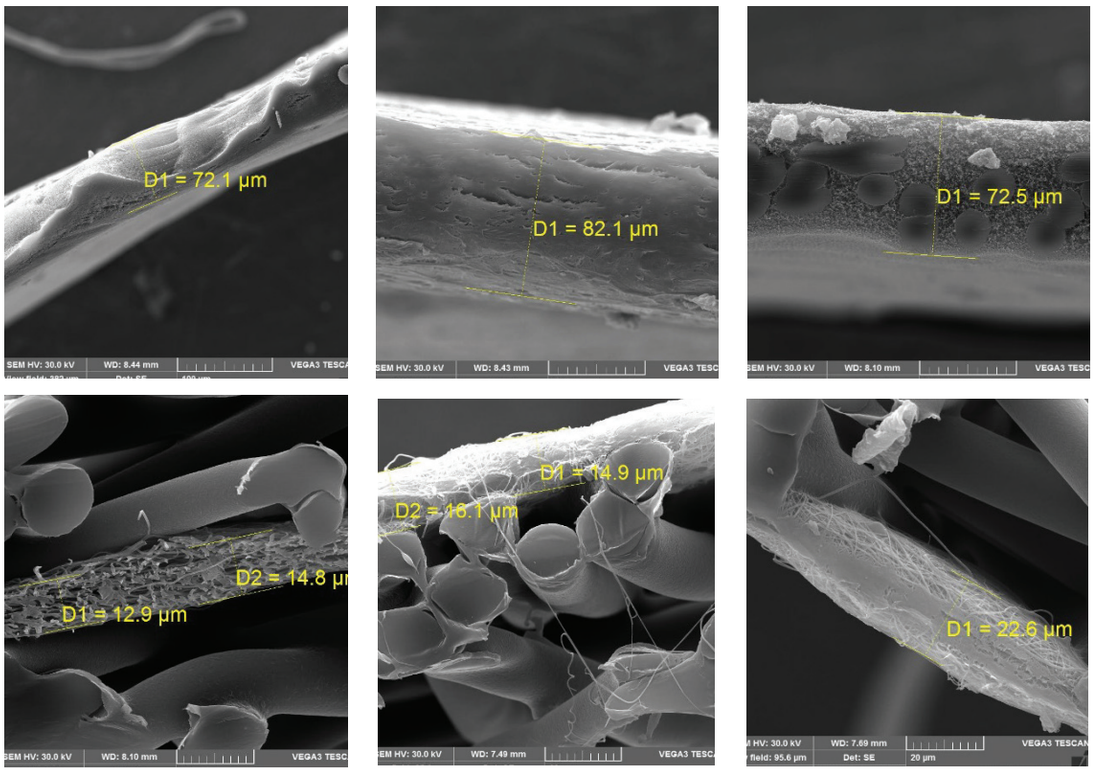

Fig. 2. Membrane cross-sections (first row, left to right: PTFE 1000×, PE 1000×, PES 500×; second row: 2PVDF139 2000×, 1PVDF155 2000×, 1PVDF226 2000×).

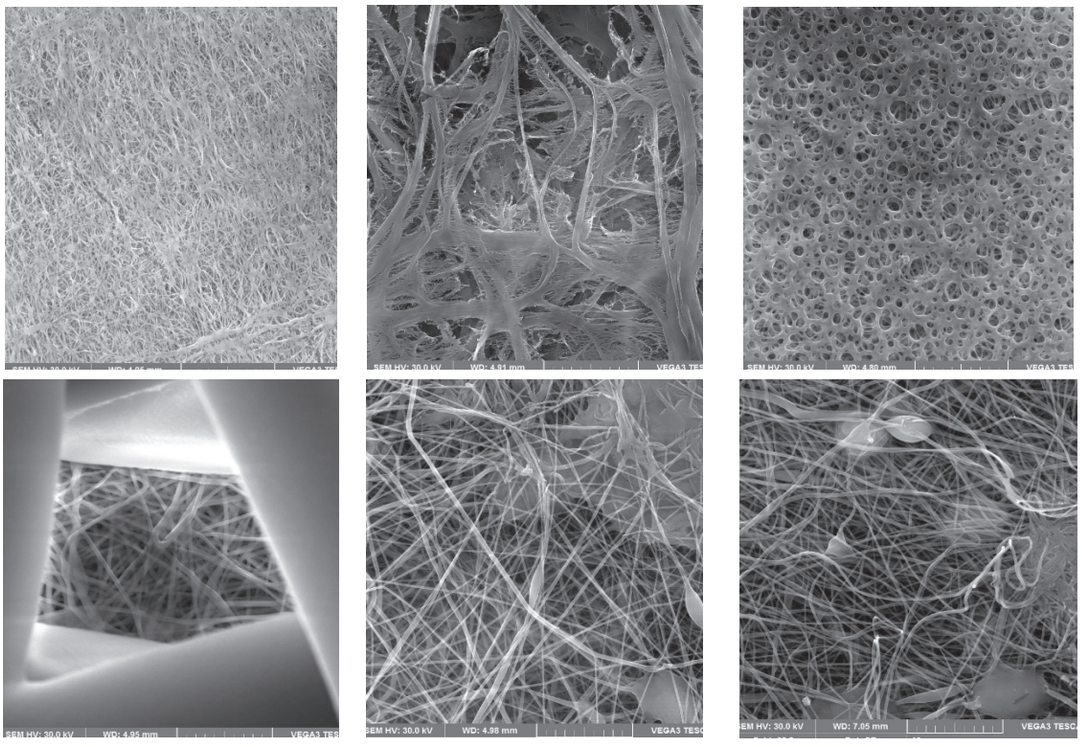

Fig. 3. Perpendicular SEM micrographs of membrane structure at 1000× (first row, left to right: PTFE, PE and PES; second row: 2PVDF139, 1PVDF155 and 1PVDF226).

3.3. Energy efficiency

Energy efficiency should increase at higher cross-flow velocities as the effective heat of condensation increases with flux, whereas the losses through conduction remain about the same. This is to be expected as the driving force is set according to LMTD, which accounts for all four inlet and outlet temperatures and not only that for the feed and distillate ΔT. On a small module, however, the temperature profile was not as developed as that on a larger module; hence, almost no efficiency increase was observed in any of the layers tested (Fig. 4B). Despite the limits inherent in the experimental setup used for estimates of energy efficiency (as reflected by a PTFE value higher than 100%), there were clear differences between the experimental films and nanofibre membranes (Fig. 4B). Considering that the thermal conductivity of PTFE (0.25 W m^{-1} K^{-1}) was similar to that for PVDF (0.19 W m^{-1} K^{-1}), the asymmetry must have been due to differences in the structure of the thicker film membranes, which also have smaller pores and excellent hydrophobicity in terms of bubble point pressure. As regards large-scale application, however, this may not be such a drawback as MD is generally driven by cheap low-grade waste heat and the low flux rates of present-day membranes may be a more significant disadvantage than mediocre energy efficiency.

3.4. Retention rate

Two aspects are of importance as regards membrane retention, i) whether feed concentration affects distillate purity, and ii) whether feed concentration reduces membrane flux. Most of the membranes tested had excellent retention rates of above 99 % (Fig. 5A), the only exception being 2PVDF139 which had a retention rate of around 85% at the highest feed concentration (displayed in Fig. 5B, together with PTFE, due to differences in the y-axis). Nanofibre membrane retention was affected by feed concentration to a greater degree than the film membranes, causing clear differences in behaviour despite their excellent retention properties. The structure of the nonwoven layers in each membrane differed, particularly as regards a wider pore size distribution (see maximum and mean pore size in Table 1) and occasional imperfections that could cause salt to penetrate from the feed to the distillate. This was not caused by membrane wetting, however, as the demineralised water flux before and after the test remained unchanged. Hence, the lamination step not only affects membrane flux and energy efficiency negatively, it also reduces membrane salt retention.

The effect of feed concentration on membrane flux was similar in both nanofibre (Fig. 6A) and film membranes (Fig. 6B), though this was probably more a function of decreasing water activity than of membrane properties. The only

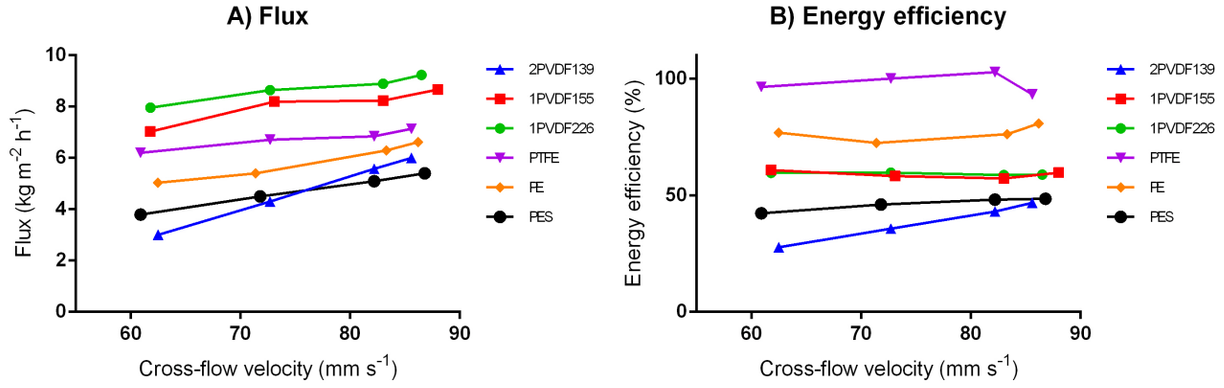

Fig. 4. A) Effect of cross-flow velocity on demineralised water flux. B) Effect of cross-flow velocity on energy efficiency.

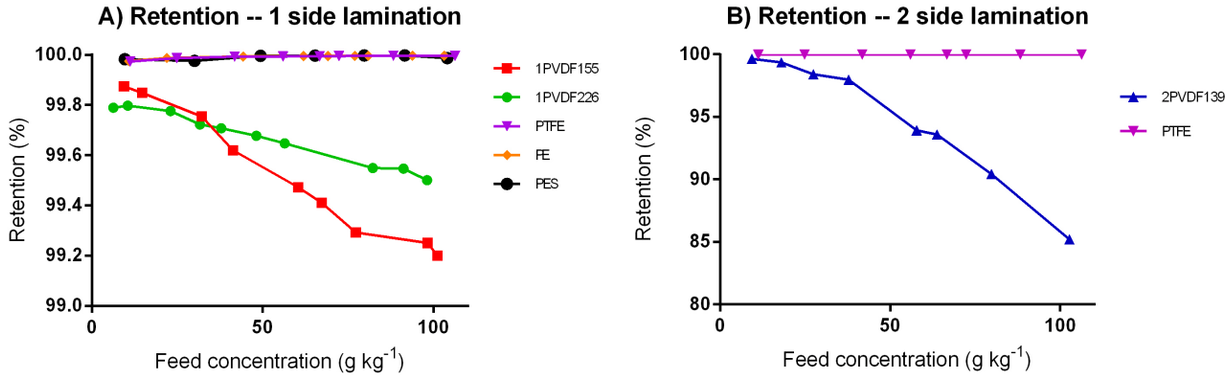

Fig. 5. Membrane retention of nanofibre film membranes with A) 1-side lamination and B) 2-side lamination.

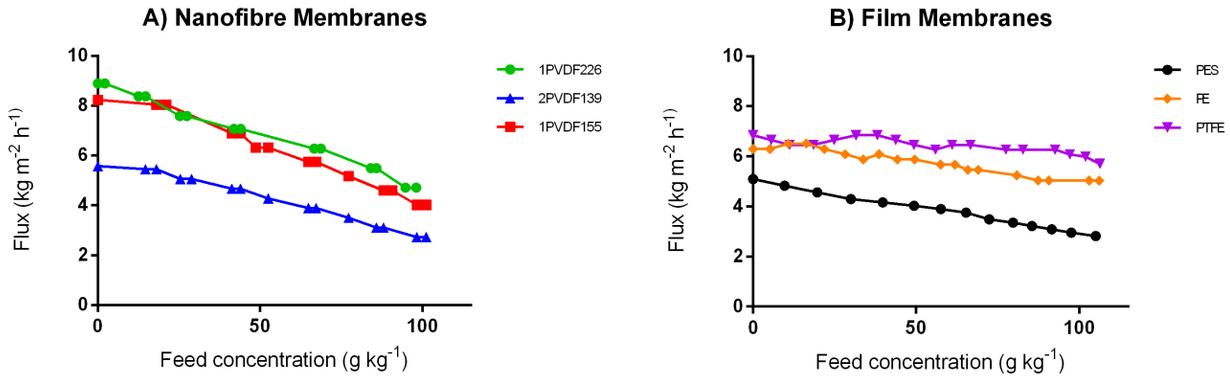

Fig. 6. Effect of feed concentration on membrane flux by A) nanofibre membranes and B) film membranes.

exception was the PTFE membrane, which appeared to be least affected and showed highest flux rates at 100 g kg^{-1}. In accordance with the observations using demineralised water (Fig. 4), 2PVDF139 and PES exhibited lowest flux rates (Fig. 6A & B).

4. Conclusions

Membrane thickness proved to be a crucial parameter when high flux rates were of most importance. While the nanofibre membranes had unrivaled permeability at all cross-flow velocities, the film membranes also displayed useful properties, with PTFE in particular easily demonstrating highest energy efficiency and greater flux rates at higher salinities than any other membrane tested. This no doubt reflects the decades of development that have already been put into the PTFE membranes.

Selection of the most appropriate membrane is crucial in the MD process, final choice depending strongly on its end use. Previous studies have confirmed that thinner PVDF membranes of up to 50 g kg^{-1} display higher permeability for saline water [16]; however, as feed salinity increases then PTFE membranes are undoubtedly better. Under present conditions, if treated solutions are beyond the range of RO due to high osmotic pressure then PTFE would be the right choice. If, on the other hand, dilute solutions are treated and high flux rates are crucial, then nanofibre membranes may prove more appropriate. Typically, any treatment of brackish or very hard groundwater will show a bottleneck in overall hydraulic performance. Power plants and other industrial facilities that produce plentiful waste heat and require softened cooling or process water (usually prepared from surface water) are promising sites for application of these new membranes.

Flux, thermal efficiency and distillate purity are all closely related and one cannot be increased without sacrificing the others. At present, the greatest requirement in MD is for increased flux rates. While nanofibre membranes clearly offer a promising solution, further improvements in membrane hydrophobicity are required before any large-scale applications can be considered. As the lamination step clearly depresses all aspects of membrane performance, and its only advantage is in increasing the membrane's physical robustness, further research should focus on the preparation of thicker nanofibre membranes that maintain the unique properties of electrospun layers without the need for support.

Abbreviations and Symbols

N	—	Flux, kg m^{-2} h^{-1}
C	—	Permeability, kg m^{-2} h^{-1} bar^{-1}
Δp	—	Vapour pressure difference, bar
E	—	Energy efficiency, %
ΔH	—	Enthalpy of condensation, J kg^{-1}
A	—	Membrane area, m^2
m	—	Mass flowrate, kg s^{-1}
C_p	—	Heat capacity at constant pressure, J kg^{-1} K^{-1}
ΔT	—	Temperature difference, °C
LMTD	—	Logarithmic mean temperature difference, °C
a_w	—	Activity of water, l
R	—	Retention, %
C_f	—	Feed concentration, g kg^{-1}
C_d	—	Distillate concentration, g kg^{-1}
DCMD	—	Direct contact membrane distillation
DMF	—	Dimethylformamide
MD	—	Membrane distillation
PTFE	—	Polytetrafluoroethylene
PE	—	Polyethylene
PES	—	Polyethersulphone
PP	—	Polypropylene
PVDF	—	Polyvinylidene fluoride
RO	—	Reverse osmosis

Acknowledgements

These results were achieved under the framework of Project LO1418 of the "Progressive development of Membrane Innovation Centre", supported under Program NPU I of the Ministry of Education, Youth and Sports of the Czech Republic, while using the infrastructure of the Membrane Innovation Centre.

The research was also supported by the Ministry of Education, Youth and Sports under the framework of targeted support under "National Programme for Sustainability I" LO 1201 and the OPR & DI project "Centre for Nanomaterials, Advanced Technologies and Innovation", CZ.1.05/2.1.00/01.0005.

References

[1] E. Drioli, A. Ali, F. Macedonio, Membrane distillation: Recent developments and perspectives, Desalination, 356 (2015) 56–84.

[2] U.K. Kesieme, N. Milne, H. Aral, C.Y. Cheng, M. Duke, Economic analysis of desalination technologies in the context of carbon pricing, and opportunities for membrane distillation, Desalination, 323 (2013) 66–74.

[3] B.L. Pangarkar, M.G. Sane, M. Guddad, Reverse osmosis and membrane distillation for desalination of groundwater: a review, ISRN Materials Science, 2011.

[4] L. Eykens, K. De Sitter, C. Dotremont, L. Pinoy, B. Van der Bruggen, How to optimize the membrane properties for membrane distillation: a review, Indust. Eng. Chem. Res., 55 (2016) 9333–9343.

[5] S. Al-Obaidani, E. Curcio, F. Macedonio, G. Di Profio, H. Al-Hinai, E. Drioli, Potential of membrane distillation in seawater desalination: thermal efficiency, sensitivity study and cost estimation, J. Membr. Sci., 323 (2008) 85–98.

[6] F. Laganà, G. Barbieri, E. Drioli, Direct contact membrane distillation: modelling and concentration experiments, J. Membr. Sci., 166 (2000) 1–11.

[7] A. Alkhudhiri, N. Darwish, N. Hilal, Membrane distillation: a comprehensive review, Desalination, 287 (2012) 2–18.

[8] A. Razmjou, E. Arifin, G. Dong, J. Mansouri, V. Chen, Superhydrophobic modification of TiO_2 nanocomposite PVDF membranes for applications in membrane distillation, J. Membr. Sci., 415 (2012) 850–863.

[9] C. Yang, X.M. Li, J. Gilron, D.F. Kong, Y. Yin, Y. Oren, ..., T. He, CF4 plasma-modified superhydrophobic PVDF membranes for direct contact membrane distillation, J. Membr. Sci., 456 (2014) 155–161.

[10] S. Tabe, Electrospun nanofibre membranes and their applications in water and wastewater treatment, Nanotechnol. Water Treat. Purif., (2014) 111–143.

[11] R.S. Barhate, S. Ramakrishna, Nanofibrous filtering media: filtration problems and solutions from tiny materials, J. Membr. Sci., 296 (2007) 1–8.

[12] A.M. Alklaibi, N. Lior, Transport analysis of air-gap membrane distillation, J. Membr. Sci., 255 (2005) 239–253.

[13] F.A. Abu Al-Rub, F. Banat, K. Beni-Melhim, Parametric sensitivity analysis of direct contact membrane distillation, Separ. Sci. Technol., 37 (2002) 3245–3271.

[14] L. Eykens, K. De Sitter, C. Dotremont, L. Pinoy, B. Van der Bruggen, Characterization and performance evaluation of commercially available hydrophobic membranes for direct contact membrane distillation, Desalination, 392 (2016) 63–73.

[15] M.K. Souhaimi, T. Matsuura, Membrane Distillation: Principles and Applications, Elsevier, 2011.

[16] L. Eykens, I. Hitsov, K. De Sitter, C. Dotremont, L. Pinoy, I. Nopens, B. Van der Bruggen, Influence of membrane thickness and process conditions on direct contact membrane distillation at different salinities, J. Membr. Sci., 498 (2016) 353–364.

[17] M.I. Ali, E.K. Summers, H.A. Arafat, Effects of membrane properties on water production cost in small scale membrane distillation systems, Desalination, 306 (2012) 60–71.